

Nonaqueous Sol–Gel Syntheses of Microporous Manganese Oxides

Stanton Ching,* Eric J. Welch, Steven M. Hughes, and Adilah B. F. Bahadoor

Department of Chemistry, Connecticut College, New London, Connecticut 06320

Steven L. Suib

Department of Chemistry, University of Connecticut, Storrs, Connecticut 06269

Received September 7, 2001. Revised Manuscript Received December 3, 2001

Microporous manganese oxides have been prepared by nonaqueous sol–gel reactions involving tetrabutylammonium (TBA) or tetraethylammonium (TEA) permanganate and methanol in the presence of alkali cation dopants. Layered birnessite-type materials were obtained for Na⁺ and K⁺ dopants in a 0.5:1 reactant ratio with manganese. Na–birnessite was isolated in hydrated and dehydrated forms (7 vs 5.6 Å interlayer spacing) whereas only the hydrated K–birnessite was observed. Cryptomelane was generated with a K:Mn ratio of 0.25:1. Spinel manganese oxides were formed with Li⁺ dopants using 0.5:1 and 0.75:1 Li:Mn ratios. The materials were characterized by powder X-ray diffraction (XRD), elemental analyses, Mn oxidation state determination, thermogravimetric analysis, and scanning electron microscopy. Thin films of manganese oxides were prepared by spin coating TEAMnO₄-derived sols onto glass slides. Unlike the bulk gel syntheses, only layered birnessite phases were obtained for thin films with Li⁺, Na⁺, and K⁺ dopants. Aerogels of K–birnessite and cryptomelane were prepared by supercritical fluid extraction of bulk gels with carbon dioxide. Surface areas were increased over the conventional sol–gel workup, but overall the values were not exceptional in these preliminary experiments.

Introduction

Microporous manganese oxides represent a large class of materials that have layered and tunneled structures consisting of edge-shared MnO₆ octahedral units. They have attracted considerable interest due to broad potential applications in heterogeneous catalysis, chemical sensing, toxic wastewater treatment, and rechargeable battery technology.^{1,2} Some of the most widely studied manganese oxides are birnessites, cryptomelane, and spinels, which are mixed-valent systems that host interstitial cations.^{1,2} The layered and tunneled structures of birnessite and cryptomelane are shown in Figure 1. In birnessite, the interlayer distance is approximately 7 Å and the gallery region is occupied by cations (typically Na⁺ and K⁺) and water molecules. Cryptomelane tunnels consist of 2 × 2 arrays of MnO₆ units and contain interstitial K⁺. The LiMn₂O₄ spinel system has been extensively studied because of its attractiveness as a low-cost and environmentally benign cathode material for rechargeable batteries.^{3–5} The spinel structure has a three-dimensional framework of edge-shared MnO₆ octahedra derived from a cubic close-packed arrangement of oxygen anions. Manganese cations are found in one-half of the octahedral holes

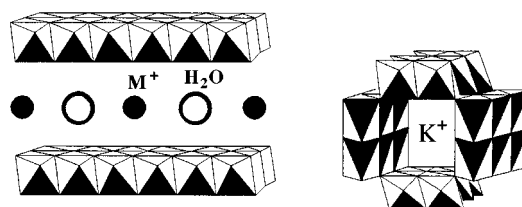


Figure 1. Structures of layered birnessite and tunneled cryptomelane. The interstitial cation in birnessite is most commonly Na⁺ or K⁺.

while lithium cations occupy one-eighth of the tetrahedral holes.

Birnessite, cryptomelane, and spinel-type manganese oxides have been prepared in varying compositions using a wide range of methods. Moreover, seemingly minor modifications have been shown to induce significant changes in properties. For example, synthetic birnessites that differ in terms of interstitial cation content, interlayer hydration, and Mn valency have shown variations in framework stability and ion-exchange capability.^{6–8} For cryptomelane, different synthetic routes have had an impact on thermal stability,^{9–11} and isomorphous doping of foreign cations

(1) Feng, Q.; Kanoh, H.; Ooi, K. *J. Mater. Chem.* **1999**, *9*, 319.

(2) Brock, S. L.; Duan, N.; Tian, Z. R.; Giraldo, O.; Zhou, H.; Suib, S. L. *Chem. Mater.* **1998**, *10*, 2619.

(3) Whittingham, M. S.; Zavalij, P. Y. *Solid State Ionics* **2000**, *131*, 109.

(4) Thackeray, M. M. *J. Am. Ceram. Soc.* **1999**, *82*, 3347.

(5) Manthiram, A.; Kim, J. *Chem. Mater.* **1998**, *10*, 2895.

(6) Strobel, P.; Charenton, J. C. *Rev. Chim. Miner.* **1986**, *23*, 125.

(7) Ching, S.; Landrigan, J. A.; Jorgensen, M. L.; Duan, N.; Suib, S. L.; O'Young, C. L. *Chem. Mater.* **1995**, *7*, 1604.

(8) Ching, S.; Petrovay, D. J.; Jorgensen, M. J.; Suib, S. L. *Inorg. Chem.* **1997**, *36*, 883.

(9) Duan, N.; Suib, S. L.; O'Young, C. L. *J. Chem. Soc., Chem. Commun.* **1995**, 1367.

into the tunneled framework has been shown to affect catalytic activity.^{12–14} Spinel manganese oxides have been prepared with many different compositions, giving rise to variations in Li⁺ content, thermal stability, and electrochemical characteristics.^{3–5,15}

The diversity of chemical and physical properties in microporous manganese oxides has been a strong driving force behind the efforts to develop new synthetic routes to these materials. Successful strategies have included solid-state reactions, molten salt processes, redox precipitation reactions, hydrothermal treatment, and sol–gel processes.^{1,2} Of these methods, the sol–gel process has been very intriguing because of its unconventional approach. Traditional sol–gel methods have employed hydrolysis and condensation reactions of metal alkoxides or hydrated metal cations to promote gel formation.^{16–18} Such procedures have been widely used to prepare solid-state metal oxides and semi-metal oxides under mild conditions. However, this approach has been stymied in the sol–gel synthesis of manganese oxides due to a lack of suitable Mn(IV) molecular precursors.¹⁹ As a consequence, nontraditional sol–gel routes have been developed using redox reactions between permanganate and organic reducing agents.

Though unrecognized as such at the time, the sol–gel chemistry of manganese oxides was first reported by Witzmann in 1915 when MnO₂ “jellies” were described in redox reactions between KMnO₄ and small saccharides such as glucose and sucrose.²⁰ More research on this system followed, but without further workup or characterization of the sol–gel products.^{21–23} In 1990, Bach and co-workers published the first account of a fully characterized microporous manganese oxide system using sol–gel methodology.¹⁹ The gels were generated by redox reactions between alkali metal permanganates and fumaric acid. Subsequent drying and calcination of the gels yielded layered and spinel phases which were examined for their structural, ion-exchange, and electrochemical characteristics.^{24–26} Similar procedures have since been reported for other syntheses of manganese oxides with layered and tunneled structures.^{7–10} The chemical reduction of alkylammonium permanganates has also been used to gen-

erate colloidal manganese oxide nanoparticles which form gels through aggregation.^{27–29}

Our work with sol–gel-derived manganese oxides began with a reinvestigation of the early findings of Witzmann. We discovered that birnessite can be obtained by calcining the xerogels obtained from reactions between KMnO₄ or NaMnO₄ with saccharides and other polyalcohols.^{7,8} Gelation occurred only if there was a suitable density of hydroxyl groups on the organic reactants, leading to the proposal that the gel matrix forms via cross-linking of manganese oxide sites by partially oxidized organic fragments. In the sol–gel reactions involving KMnO₄, we also demonstrated that partial extraction of K⁺ from the gel matrix promoted the formation of cryptomelane.^{8–10}

Previous sol–gel syntheses of microporous manganese oxides have been carried out in aqueous media or water–alcohol mixtures. We have been investigating reactions in nonaqueous media in an effort to broaden the scope of manganese oxide sol–gel chemistry and to better exploit some of the advantages of sol–gel processing. Our goals have been to compare the aqueous and nonaqueous sol–gel chemistry and to develop methods of preparing these materials in different forms, such as thin films and aerogels. Here, we report the first nonaqueous sol–gel syntheses of microporous manganese oxides and our initial studies on the preparation of thin films and aerogels.

Experimental Section

Chemicals. Reagent-grade chemicals were obtained commercially and used without further purification. Tetrabutylammonium (TBA) bromide was obtained from Fluka. Tetraethylammonium (TEA) chloride was obtained from Aldrich, as were potassium acetate, sodium acetate, and lithium acetate dihydrate. KMnO₄ was obtained from Fisher. Distilled deionized water was obtained from a Barnsted Nanopure II water-purifying system and used throughout. TBAMnO₄ and TEAMnO₄ were prepared by metathesis reactions between KMnO₄ and alkylammonium halides in water.³⁰ The compounds were dried under vacuum at room temperature and stored in refrigeration to limit thermal decomposition. TBAMnO₄ and TEAMnO₄ are not considered explosion hazards, as are other permanganate salts with unsaturated organic cations, but as a general precaution they were never handled above ambient temperature.

General Synthetic Procedure for Microporous Manganese Oxides. The following procedure is used to prepare Na–birnessite, K–birnessite, cryptomelane, and spinel manganese oxides. TBAMnO₄ is used in this case, but TEAMnO₄ works equally well. A 0.40-g (1.1-mmol) sample of TBAMnO₄ was added to 6 mL of 0.090 M alkali metal acetate (0.045 M for cryptomelane and 0.14 M also used in spinel preparation). The dark purple solution was mixed thoroughly and stoppered. The sol turned reddish after 10–15 min and then dark brown after about 40 min. A monolithic brown gel formed after 45–90 min of reaction at room temperature. The gel was allowed to stand overnight and the expelled methanol was decanted. After further drying at 110 °C for 24 h, the resulting xerogel was calcined at 450 °C for 2 h to yield the manganese oxide product as a black powder. The product was washed three

(10) Ching, S.; Roark, J. L.; Duan, N.; Suib, S. L. *Chem. Mater.* **1997**, *9*, 750.

(11) DeGuzman, R. N.; Shen, Y. F.; Neth, E. J.; Suib, S. L.; O'Young, C. L.; Levine, S.; Newsam, J. M. *Chem. Mater.* **1994**, *6*, 815.

(12) Zhou, H.; Shen, Y. F.; Wang, J. Y.; Chen, X.; O'Young, C. L.; Suib, S. L. *J. Catal.* **1998**, *176*, 321.

(13) Xia, G. G.; Yin, Y. G.; Willis, W. S.; Wang, J. Y.; Suib, S. L. *J. Catal.* **1999**, *185*, 91.

(14) Chen, X.; Shen, Y. F.; Suib, S. L.; O'Young, C. L. *J. Catal.* **2001**, *197*, 292.

(15) Paulson, J. M.; Dahn, J. R. *Chem. Mater.* **1999**, *11*, 3065.

(16) Hench, L. L.; West, J. K. *Chem. Rev.* **1990**, *90*, 33.

(17) Brinker, C. J.; Scherer, G. W. *Sol–Gel Science*; Academic Press: San Diego, CA, 1990.

(18) Livage, J.; Henry, M.; Sanchez, C. *Prog. Solid State Chem.* **1988**, *18*, 259.

(19) Bach, S.; Henry, M.; Baffier, N.; Livage, J. *J. Solid State Chem.* **1990**, *88*, 325.

(20) Witzmann, E. J. *J. Am. Chem. Soc.* **1915**, *35*, 1079.

(21) Witzmann, E. J. *J. Am. Chem. Soc.* **1917**, *37*, 25.

(22) Cuy, E. J. *J. Phys. Chem.* **1921**, *25*, 415.

(23) Prakash, S.; Dhar, N. R. *J. Ind. Chem. Soc.* **1930**, *7*, 417.

(24) Le Goff, P.; Baffier, N.; Bach, S.; Pereira-Ramos, J. P.; Messina, R. *Solid State Ionics* **1993**, *61*, 309.

(25) Le Goff, P.; Baffier, N.; Bach, S.; Pereira-Ramos, J. P. *J. Mater. Chem.* **1994**, *4*, 875.

(26) Le Goff, P.; Baffier, N.; Bach, S.; Pereira-Ramos, J. P. *Mater. Res. Bull.* **1996**, *31*, 63.

(27) Brock, S. L.; Sanabria, M.; Suib, S. L.; Urban, V.; Thiyagarajan, P.; Potter, D. *J. Phys. Chem. B* **1999**, *103*, 7416.

(28) Brock, S. L.; Sanabria, M.; Nair, J.; Suib, S. L.; Ressler, T. *J. Phys. Chem. B* **2001**, *105*, 5404.

(29) Gao, Q.; Giraldo, O.; Tong, W.; Suib, S. L. *Chem. Mater.* **2001**, *13*, 778.

(30) Karaman, H.; Barton, R. J.; Robertson, B. E.; Lee, D. G. *J. Org. Chem.* **1984**, *49*, 4509.

times with water and dried under vacuum at room temperature. (Na–birnessite required prior overnight stirring in water to convert the dehydrated 5.6-Å phase into the hydrated 7-Å phase. Cryptomelane required three initial washings with 0.1 M HCl to remove surface-adsorbed potassium ions.) A typical isolated yield was 0.10 g.

Thin Films. Manganese oxide sols derived from TEAMnO_4 were prepared according to the procedure described above. Glass substrates (1 × 1 in.) were cleaned by sonication in aqueous Alconox detergent followed by two rounds of sonication for 30 s each in water, methanol, and acetone. Spin coating was carried out using a Chemat KW-4B spin coater. Once the sols became reddish-brown to brown in color, 7–8 drops were applied by pipet as the substrate was spun at 750 rpm for 10 s. The substrate was then spun for an additional 10 s at 1500 rpm. The light brown sol–gel films were allowed to stand in air for 1 h before being calcined at 450 °C for 2 h.

Aerogels. Gel precursors for K–birnessite and cryptomelane were prepared as described above and then transferred to a lidded trough made of stainless steel wire mesh. Supercritical drying was carried out using a SPI critical point dryer. Samples were subjected to two extractions in supercritical CO_2 for 30 min each at 35 °C and 1200 psi. If the critical point could not be reached initially, a 10-min extraction in liquid CO_2 was performed prior to supercritical treatment.

Characterization. Powder X-ray diffraction (XRD) data were collected with a Scintag 2000 PDS X-ray diffractometer using $\text{Cu K}\alpha$ radiation. Samples were spread onto glass slides and scanned at 5° 2 θ /min. The beam voltage and beam current were 45 kV and 40 mA, respectively. Electron microscopy was carried out using a LEO model 435VP scanning electron microscope. Thermogravimetric analysis (TGA) was performed using a Perkin-Elmer model TGA 7 instrument using a heating rate of 20 °C/min. Surface area measurements were obtained by BET analysis using a Micrometrics ASAP 2010 analyzer. Elemental analyses were obtained by atomic absorption spectroscopy with a Perkin-Elmer Model 2380 spectrometer using an air/acetylene flame. Average oxidation states for manganese were determined by iodometric redox titration.³¹ Chemical formulas of the manganese oxides were calculated from the combined results of elemental analyses, Mn oxidation state determination, and thermogravimetric analysis.⁸ Infrared spectra were obtained with a Perkin-Elmer model PE 16 FT-IR spectrometer using solution cells with CaF_2 windows. ¹³C NMR spectra were obtained using a Bruker AC-250 NMR spectrometer (62.86 MHz for ¹³C). Chemical shifts are reported in ppm relative to tetramethylsilane using the 20% ¹³C-enriched methanol solvent (49 ppm) as an internal reference.

Results and Discussion

Nonaqueous Sol–Gel Preparation of Manganese Oxides. Manganese oxide gels were prepared from 0.18 M solutions of tetrabutylammonium permanganate (TBAMnO_4) or tetraethylammonium permanganate (TEAMnO_4) in methanol. The sols were initially reddish, but turned brown before condensing into monolithic gels after 1–2 h. The gels were allowed to age at room temperature for 1 day before being dried at 110 °C overnight. Calcination of the resulting xerogels at 450 °C for 2 h produced manganese oxides as polycrystalline powders. The addition of alkali metal dopants as structural templates was critical for the synthesis of microporous materials. In the absence of cation dopants, the reactions between alkylammonium permanganates and methanol yielded nonporous Mn_2O_3 . Microporous manganese oxides such as birnessite, cryptomelane, and spinel were obtained only when alkali metal cations were incorporated into the gel matrix (Table 1). Metal

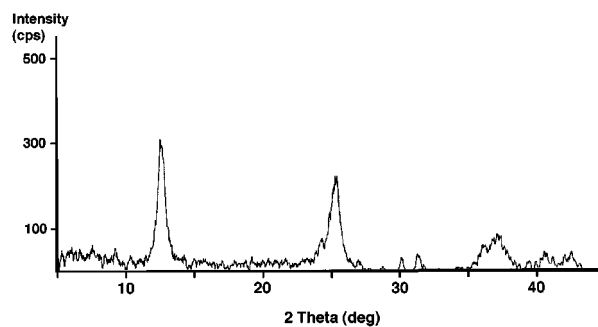


Figure 2. Powder XRD pattern of K–birnessite.

Table 1. Manganese Oxide Products from Nonaqueous Sol–Gel Reactions between Tetraalkylammonium Permanganates and Methanol

dopant cation	dopant:Mn ratio	product
none	NA	Mn_2O_3
K^+	0.5:1	K–birnessite
K^+	0.25:1	cryptomelane
Na^+	0.5:1	Na–birnessite
Li^+	0.5:1; 0.75:1	spinel

acetates were used to deliver the cations because they provided the best combination of methanol solubility and anion combustibility upon calcination. In general, the amount of dopant in the final product was about half of what was present at the beginning of the sol–gel process. The excess cation was either expelled along with methanol when the gel was aged or removed from the final product by washing after calcination. Similar situations were encountered previously in aqueous sol–gel syntheses of manganese oxides.^{8,10} These reactions used KMnO_4 and NaMnO_4 as reactants and therefore introduced alkali metals in 1:1 ratios with Mn.

Attempts to incorporate divalent cations as templates for manganese oxide structures were unsuccessful. Gels were obtained with acetate salts of Mg^{2+} , Ba^{2+} , and Cu^{2+} as dopants, but subsequent drying and calcination yielded only nonporous Mn_2O_3 . The formation of gels in the nonaqueous sol–gel system was nonetheless a notable improvement over similar experiments conducted in water where the addition of divalent cations caused the formation of flocculent and highly dispersed gels.⁸

K^+ Dopant. Gels doped with potassium ions were precursors to birnessite or cryptomelane, depending on the concentration of K^+ in the gel matrix. A 0.5:1 K:Mn ratio promoted the formation of layered K–birnessite, whereas a 0.25:1 K:Mn ratio favored tunneled cryptomelane. The two reactions were otherwise identical. The influence of K^+ content on the manganese oxide structure was previously observed in aqueous sol–gel syntheses and has been attributed to the fact that K–birnessite typically contains more than twice the interstitial K^+ as cryptomelane.^{8–10} Overall, K–birnessite and cryptomelane prepared by nonaqueous sol–gel chemistry were similar to their aqueous sol–gel counterparts.

The powder XRD pattern of K–birnessite from the 0.5:1 K:Mn sol–gel mixture is shown in Figure 2. The observed peaks corresponding to 7.02 and 3.51 Å are characteristic of layered, birnessite-type manganese oxides with a 7-Å interlayer spacing. Lower intensity peaks at 2.49, 2.42, 2.22, and 2.13 Å are also consistent with the birnessite structure. SEM images show the material to consist of irregularly shaped globules of 0.1–

(31) Murray, J. W.; Balistieri, L. S.; Paul, B. *Geochim. Cosmochim. Acta* **1984**, *48*, 1237.

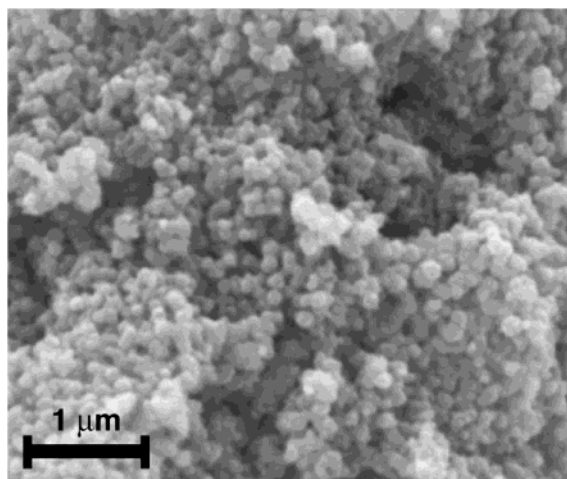


Figure 3. SEM image of K–birnessite.

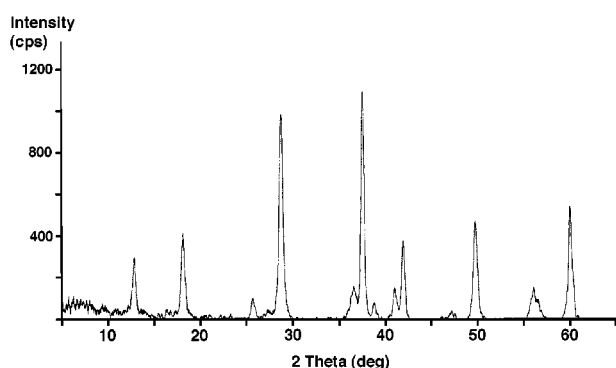


Figure 4. Powder XRD pattern of cryptomelane.

0.2- μm diameter (Figure 3). A chemical formula of $\text{K}_{0.29}\text{MnO}_{2.01}(\text{H}_2\text{O})_{0.32}$ was determined for K–birnessite from elemental analyses (10.8% K, 52.5% Mn) and the average oxidation state (3.73) of the mixed-valent Mn.^{8,10} The TGA profile showed an initial 8% decrease in weight up to 200 °C that was attributed to the loss of interlayer water. There was also a subsequent 4.5% weight loss from 730 to 900 °C due to the formation of Mn_3O_4 , which was verified by XRD. Thermal degradation of K–birnessite has been known to produce cryptomelane at about 600 °C,^{11,32} but this transformation was not apparent for the nonaqueous sol–gel system.

The formation of cryptomelane from the 0.25:1 K:Mn sol–gel mixture was confirmed by XRD (Figure 4). SEM images revealed fibrous particles that are consistent with observations from other synthetic cryptomelane materials (Figure 5). The TGA profile revealed a weight loss of <1% up to 200 °C, indicating that the tunnels were essentially free of interstitial water. A weight loss of 5% from 550 to 770 °C corresponded to the formation of Mn_2O_3 , while a final transition showing 4% weight loss from 770 to 900 °C represented the conversion to Mn_3O_4 . A formula of $\text{K}_{0.14}\text{MnO}_{1.99}$ was determined for cryptomelane based on elemental analyses (5.5% K and 59.9% Mn) and a Mn oxidation state of 3.85.

Na⁺ Dopant. A 0.5:1 Na:Mn ratio in the sol–gel reaction produced a dehydrated form of Na–birnessite (5.6-Å layer spacing) after drying and calcination.⁸ Subsequent hydration of the interlayer region produced

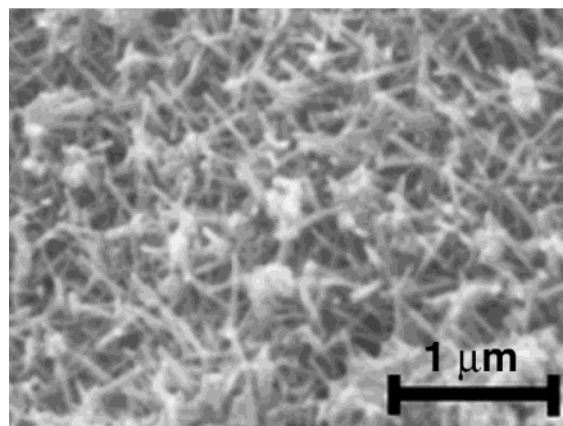


Figure 5. SEM image of cryptomelane.

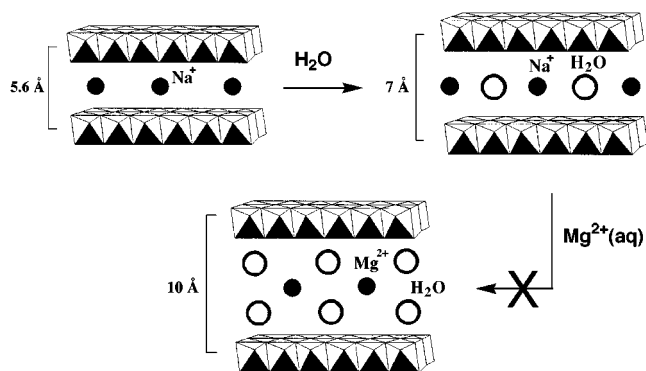


Figure 6. Reaction scheme showing the hydration of 5.6-Å Na–birnessite along the inability of the resulting 7-Å Na–birnessite to undergo ion exchange and further hydration to form 10-Å layered buserite.

the 7-Å Na–birnessite (Figure 6). Attempts to further hydrate the 7-Å birnessite into 10-Å buserite by ion exchange were unsuccessful. (Buserite is a closely related, layered manganese oxide with an additional sheet of interlayer water in the gallery region.) By contrast, Na–birnessite prepared by aqueous precipitation routes can be readily transformed into buserite through ion exchange with divalent cations such as Mg^{2+} , Co^{2+} , Ni^{2+} , Cu^{2+} , and Zn^{2+} .^{33,34}

The XRD patterns of dehydrated and hydrated sol–gel Na–birnessites are shown in Figure 7. The patterns clearly illustrate the expansion of the layers from 5.6 to 7 Å due to incorporation of interlayer water. The lack of interstitial water in 5.6-Å Na–birnessite was confirmed by TGA. Similar products were obtained from aqueous sol–gel processes with NaMnO_4 and sugars, although in those cases calcination of the xerogel at 400 °C yielded a mixture of the 5.6- and 7-Å layered phases, whereas pure 5.6-Å Na–birnessite was only obtained from direct calcination at 800 °C.⁸ SEM images of 7-Å Na–birnessite showed a particle morphology identical to that of K–birnessite, as previously shown in Figure 3.

A formula of $\text{Na}_{0.35}\text{MnO}_{2.09}(\text{H}_2\text{O})_{0.28}$ was determined for 7-Å Na–birnessite using the elemental analyses of Na (7.9%) and Mn (54.4%), along with the average Mn

(32) Chen, C. C.; Golden, D. C.; Dixon, J. B. *Clays Clay Miner.* **1986**, *34*, 565.

(33) Shen, Y. F.; Suib, S. L.; O'Young, C. L. *J. Am. Chem. Soc.* **1994**, *116*, 11020.

(34) Ching, S.; Krukowska, K. S.; Suib, S. L. *Inorg. Chim. Acta* **1999**, *294*, 123.

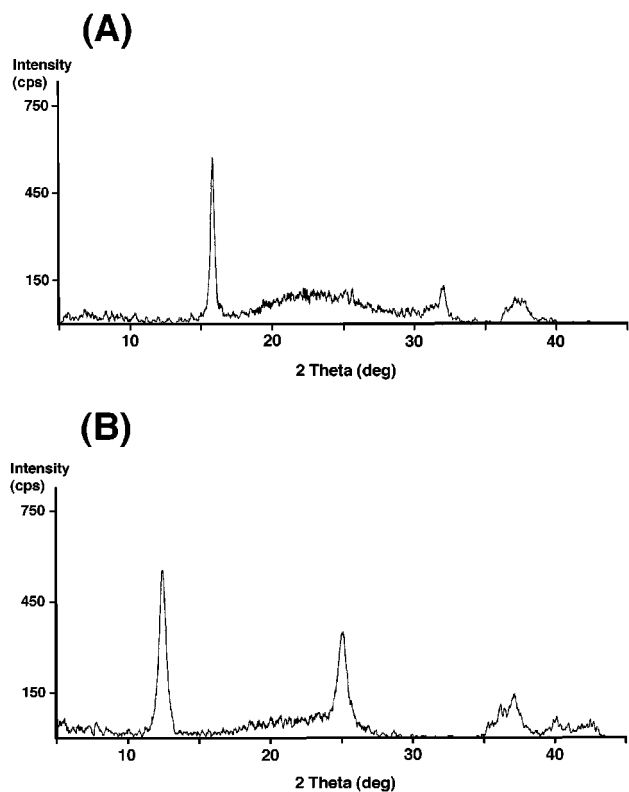


Figure 7. Powder XRD patterns of (A) dehydrated 5.6-Å Na-birnessite and (B) hydrated 7-Å Na-birnessite.

oxidation state of 3.83. The Mn oxidation state was the same in 5.6-Å Na-birnessite, indicating that hydration occurred without oxidizing the manganese oxide framework. By contrast, an aqueous NaMnO_4 /fumaric acid sol-gel route produces Na-birnessite in which Mn undergoes oxidation during a similar conversion.²⁴ In that synthesis, a 5.5-Å layered phase was initially produced, $\text{Na}_{0.7}\text{MnO}_{2.14}(\text{NaOH})_{0.3}$, with an average Mn oxidation state of 3.58. Subsequent hydration then gave a 7-Å Na-birnessite phase, $\text{Na}_{0.45}\text{MnO}_{2.14}(\text{H}_2\text{O})_{0.76}$, as Na^+ was extracted and Mn in the framework was oxidized to an average valence of 3.83. The average Mn oxidation states for nonaqueous sol-gel Na-birnessite and K-birnessite are consistent with the values of 3.6–3.8 typically reported for layered manganese oxides prepared by permanganate oxidation of organic molecules.^{8,19,24,35} However, these values are generally higher than the average oxidation state range of 3.5–3.7 observed in birnessites prepared by aqueous precipitation methods.^{6,34,36,37}

The TGA profile of 7-Å Na-birnessite (Figure 8) showed a weight loss of 5% up to 200 °C that was assigned to the loss of interlayer water. This agreed with the value of 4.6% determined from elemental analysis and oxidation state data. However, despite the facile water loss, attempts to generate 5.6-Å Na-birnessite by dehydrating 7-Å birnessite were unsuccessful. Heat treatment of 7-Å Na-birnessite at 200 °C yielded amorphous manganese oxide. Thus, it appears the crystallinity of the layered framework is sufficiently

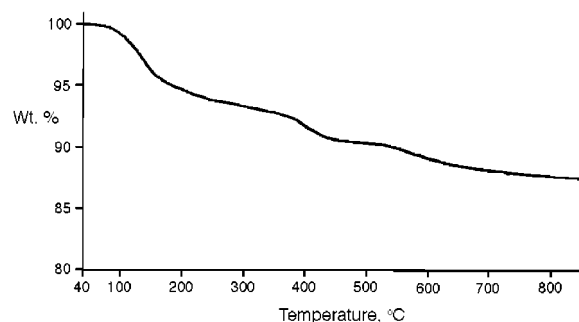


Figure 8. TGA profile of 7-Å Na-birnessite.

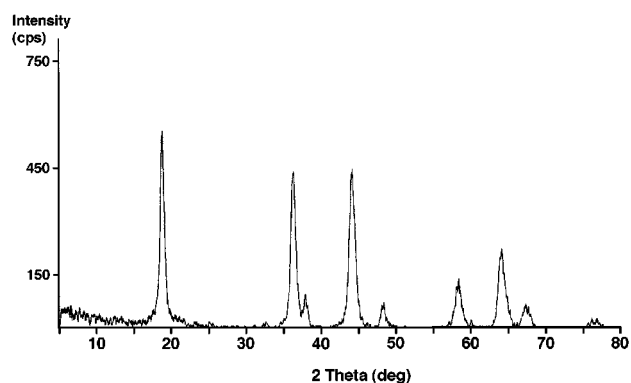


Figure 9. Powder XRD pattern of spinel manganese oxide using a 0.5:1 Li:Mn ratio in the nonaqueous sol-gel preparation. The same pattern is observed using a 0.75:1 Li:Mn ratio.

fragile that dehydration, even at modest temperatures, causes the structure to become disordered. Further inspection of the TGA profile revealed an unidentified transition at about 380 °C associated with the amorphous manganese oxide. The final weight loss beginning at 540 °C was due to the formation of Mn_3O_4 . Thermal analysis therefore indicated that the nonaqueous sol-gel Na-birnessite was less stable than birnessites synthesized by other methods.

The inability of the 7-Å Na-birnessite to revert to its dehydrated precursor was similarly observed for sol-gel Na-birnessite prepared from NaMnO_4 and sugars in aqueous solution.⁸ However, another aqueous sol-gel reaction involving NaMnO_4 and fumaric acid produced Na-birnessite that was readily interconverted between the 7- and 5.6-Å phases.²⁴ The differences in these systems underscore the observation that seemingly small variations in preparation method, composition, and structure can result in significant variations in manganese oxide properties.

Li⁺ Dopant. Spinel manganese oxides were generated from sol-gel reactions in the presence of Li⁺ dopants. Monolithic gels were obtained using Li:Mn ratios of 0.5:1 and 0.75:1. At higher ratios, the gels became flocculent. Calcined xerogels yield spinels having the characteristic XRD pattern shown in Figure 9. SEM images showed particles with irregular shapes and varying sizes (Figure 10). On the basis of elemental analyses, the manganese oxides were Li-deficient spinels with compositions of $\text{Li}_{0.60}\text{Mn}_2\text{O}_{3.86}$ for the 0.5:1 Li:Mn ratio and $\text{Li}_{0.82}\text{Mn}_2\text{O}_{4.16}$ for the 0.75:1 ratio (Table 2). The average Mn oxidation states of 3.56 and 3.75 calculated from these formulas compared favorably to the values of 3.59 and 3.71 determined experimentally by iodometric redox titration.

(35) Ma, Y.; Luo, J.; Suib, S. L. *Chem. Mater.* **1999**, *11*, 1972.

(36) Feng, Q.; Yanagisawa, K.; Yamasaki, N. *J. Mater. Sci. Lett.* **1997**, *16*, 110.

(37) Luo, J.; Zhang, Q.; Suib, S. L. *Chem. Mater.* **2000**, *39*, 741.

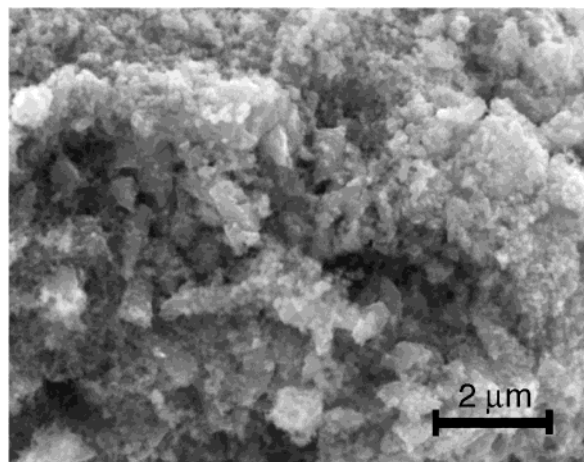


Figure 10. SEM image of spinel manganese oxide.

Table 2. Analytical Data for Spinel-Type Manganese Oxides Prepared by the Nonaqueous Sol–Gel Process

Li:Mn ratio (reactants)	% Li ^a	% Mn ^a	% O ^b	ox. st. ^c	chemical formula
0.5:1	2.37	62.5	35.1	3.56 (3.59)	Li _{0.60} MnO _{3.86}
0.75:1	3.12	60.3	36.6	3.75 (3.71)	Li _{0.82} Mn ₂ O _{4.16}

^a Determined by atomic absorption spectroscopy. ^b Determined from % Li and % Mn by difference. ^c Calculated from elemental percentages (determined by iodometric redox titration).

Most manganese oxide spinels have compositions close to the ideal formula of LiMn₂O₄, representing a structure of cubic close-packed oxygen with manganese in one-half of the octahedral holes and Li⁺ in one-eighth of the tetrahedral holes. In the nonaqueous sol–gel system, it appears the deficiency of Li⁺ in the gel matrix still provides adequate templating for the spinel structure. The lower interstitial Li⁺ concentration has been compensated by an increase in the average Mn oxidation state. The loss of significant amounts of Li⁺ dopant also indicates that the cations are not tightly bound in the sol–gel matrix.

Other sol–gel routes are known for manganese oxide spinels. Chelation of Mn²⁺ by adipic acid³⁸ or poly(vinyl butyral)³⁹ in the presence of Li⁺ has been shown to produce gels in the form of viscous, polymeric resins. However, long 10-h calcination is required to convert the gels into spinel manganese oxides. A redox reaction between permanganate and fumaric acid has also proven successful, using either LiMnO₄ or stoichiometrically precise H_{0.5}Li_{0.5}MnO₄ as a precursor to prepare the LiMn₂O₄ spinel.^{24,40}

Nonaqueous Sol–Gel. The nonaqueous sol–gel process produced monolithic gels from the reduction of TBAMnO₄ or TEAMnO₄ in methanol. In related aqueous reactions between permanganate and polyfunctionalized organic reducing agents, the gel was presumably formed through cross-linking of manganese oxide sites by partially oxidized organic fragments.⁸ Indeed, the oxidation of methanol by permanganate in aqueous solution yielded precipitates rather than gels, which is

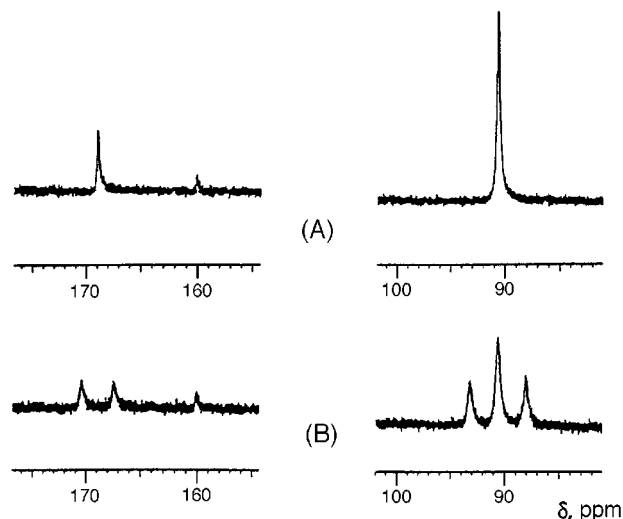


Figure 11. ¹³C NMR spectra of a nonaqueous gel prepared from an undoped reaction of TBAMnO₄ in 20% ¹³C-enriched methanol: (A) ¹H-decoupled, (B) ¹H-coupled. Large signals from the methanol solvent and TBA cation have been omitted for clarity.

consistent with the need for a cross-linking mechanism. However, attempts to improve the nonaqueous sol–gel process by adding polyalcohols as cross-linking reagents proved detrimental. Reagents such as ethylene glycol and glycerol, which were effective at promoting gelation in aqueous systems, produced poor quality gels when added to permanganate/methanol mixtures. The resulting gels were either flocculent or tainted with grainy particulates. Similar difficulties were encountered when polyalcohols were reacted with alkylammonium permanganates in other organic solvents, including different alcohols. Thus, it appears the formation of a nonaqueous gel matrix is not directly analogous to its aqueous counterpart.

¹³C NMR spectra of nonaqueous gels prepared with 20% ¹³C-enriched methanol were fairly uncomplicated. The spectra were dominated by resonances from the methanol solvent and alkylammonium cation, but otherwise just three other resonances of much lower intensity were observed (Figure 11). The doublet at 168.7 ppm with C–H coupling of 214 Hz was assigned to formate ion. FT-IR spectroscopy on the gel confirmed the assignment with the detection of a carbonyl band at 1618 cm⁻¹, the same as sodium formate alone in methanol. The very weak singlet at 160.1 ppm was believed to be due to carbonate ion. A much stronger triplet at 90.4 ppm showing 195-Hz C–H coupling was consistent with the presence of paraformaldehyde oligomers, which are reasonable byproducts of methanol oxidation.

The nature of the manganese oxide gel matrix remains speculative. One possibility is that the manganese oxide sites are cross-linked by bridging formate or paraformaldehyde oligomers, although this is based on solution-phase species trapped in the gel. Unfortunately, potentially useful NMR signals from carbon atoms in bonding proximity to manganese would be suppressed by paramagnetic Mn(III) and Mn(IV). Another possibility is that gelation is induced by an increase in solution viscosity due to aggregation of manganese oxide particles. Gels have been shown to form from crystalline

(38) Lee, Y. S.; Sun, Y. K.; Nahm, K. S. *Solid State Ionics* **1998**, *109*, 285.

(39) Sun, Y. K.; Oh, I. H.; Choi, J. G. *J. New Mater. Electrochem. Syst.* **1999**, *2*, 50.

(40) Bach, S.; Farcy, J.; Pereira-Ramos, J. P. *Solid State Ionics* **1998**, *110*, 193.

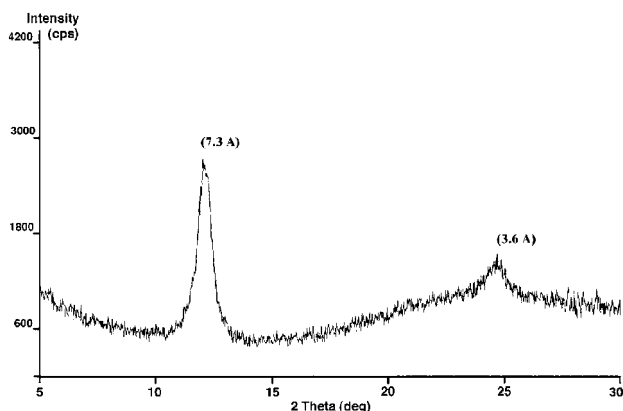


Figure 12. Powder XRD pattern of a Li-birnessite thin film on glass. The film was prepared by spin coating a Li⁺-doped, sol-gel mixture of TEAMnO₄ in methanol (0.5:1 Li:Mn ratio) followed by calcination at 450 °C.

manganese oxide nanoparticles in aqueous solutions with up to 20% 2-butanol.^{27–29} Although, crystallinity has not been observed in the methanolic gels, there is still the potential for gelation from amorphous aggregates.

Thin Films and Aerogels. Preliminary experiments were carried out on the preparation of manganese oxide thin films and aerogels, which we considered excellent targets for the nonaqueous sol-gel process. For thin films, nonaqueous sols offer superior substrate wetting over aqueous solutions and therefore should promote more homogeneous and well-formed films. The methanol sols are also stable for 1–2 h, making them much easier to work with than analogous aqueous sols, which undergo gelation within minutes. For aerogels, methanol can be extracted from gels with supercritical carbon dioxide without pretreatment. Water, by comparison, is immiscible with supercritical CO₂, so aqueous gels require a solvent-exchange step prior to supercritical drying.

Spin-coated films were prepared using sol-gel reactions with both TBAMnO₄ and TEAMnO₄ in methanol. Light brown, evenly coated films were obtained for both undoped and cation-doped sol-gels after calcination. XRD analyses of the calcined thin films revealed significant differences from the synthesis of bulk gels. The undoped films were amorphous, compared to the generation of Mn₂O₃ in bulk samples. Cation-doped films (K⁺, Na⁺, Li⁺) from TBAMnO₄/methanol sol-gels (0.5:1 dopant:Mn) were similarly amorphous, although a very faint diffraction peak near 7 Å was occasionally observed. By contrast, cation-doped films from TEAMnO₄/methanol sol-gels all yielded XRD patterns with peaks at 7 and 3.5 Å that were characteristic of layered, birnessite-type manganese oxides. Unlike syntheses of bulk gels, cryptomelane was not formed when a 0.25:1 K:Mn ratio was used, nor was there evidence of spinel phase for 0.5:1 or 0.75:1 Li:Mn ratios. The XRD pattern of a Li-birnessite thin film is shown in Figure 12. Similar patterns were observed for Na-birnessite and K-birnessite films. Also, for Na-birnessite thin films, the 5.6-Å dehydrated phase was not observed.

The preferential formation of layered birnessite structures in thin films bears resemblance to epitaxial film growth on single-crystal substrates. However, the match between the film material and substrate is clearly less

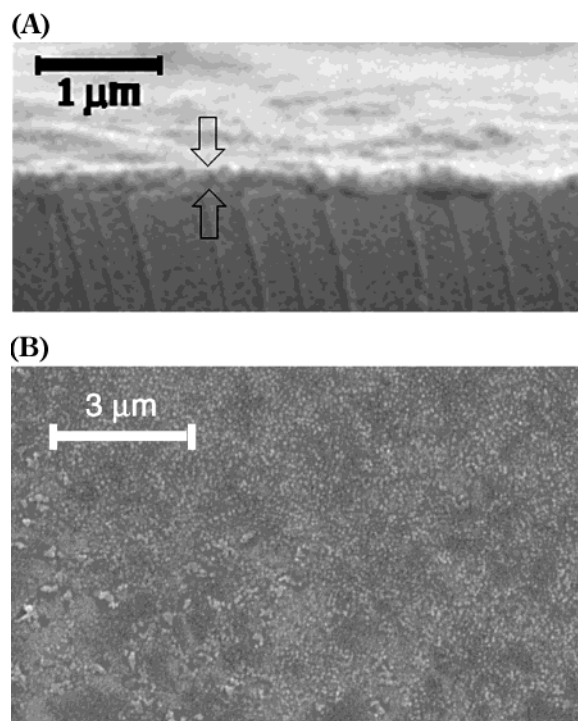


Figure 13. SEM images of a sol-gel-derived Li-birnessite thin film. (A) Edge view showing a thickness of approximately 0.2 μm. (B) Top view.

critical in this case. SEM analyses of the thin films showed well-formed surfaces that consisted of submicrometer-sized globular particles (Figure 13). This morphology was also observed in bulk samples of Na- and K-birnessite, shown previously in Figure 3. The film thickness of 0.1–0.2 μm is characteristic of sol-gel coatings.⁴¹

The difference in crystallinity between thin films derived from TEAMnO₄ and TBAMnO₄ is attributed to a higher density of manganese oxide material in the TEAMnO₄-derived films since TEA⁺ is significantly smaller than TBA⁺. The manganese oxide sites need to be in closer proximity to properly crystallize in a thin film gel, given that less material is present compared to a bulk gel. Interestingly, the differences in thin film quality are not obvious from examination by SEM.

Sol-gel chemistry has been used previously to prepare manganese oxide thin films, but with aqueous solvent. The reaction between KMnO₄ and sucrose has been shown to generate K-birnessite films on glass by immersion, spray, and spatula coating methods.⁴² These films had thickness on the order of 1 μm. Thinner films of approximately 0.5 μm were obtained by spin coating, but this technique yielded amorphous films. In terms of surface appearance, the films were rougher than those reported here for the nonaqueous sol-gel route. Reduction of aqueous permanganate by fumaric acid has also been used to prepare aqueous gels or colloids that served as precursors for MnO₂ thin films.^{43–45} These

(41) Francis, L. F. In *Intermetallic and Ceramic Coatings*; Dahotre, N. B., Sudarshan, T. S., Eds.; Materials Engineering Series Volume 13; Marcel Dekker: New York, 1999; pp 31–82.

(42) Segal, S. R.; Park, S. H.; Suib, S. L. *Chem. Mater.* **1997**, *9*, 98.

(43) Städtnychuk, H. P.; Anderson, M. A.; Chapman, T. W. *J. Electrochem. Soc.* **1996**, *143*, 1629.

(44) Pang, S. C.; Anderson, M. A.; Chapman, T. W. *J. Electrochem. Soc.* **2000**, *147*, 444.

systems have been studied as possible thin film cathodes or ultracapacitors. Crystalline manganese oxide colloids have also been used to cast drop-coated films of about 1- μm thickness onto glass substrates.⁴⁶ These thin films were distinct in their ability to undergo fast ion-exchange reactions with both organic and inorganic cations.

An aerogel route was explored as a way to prepare high surface area K–birnessite and cryptomelane from TBAMnO₄-derived gels. Procedures were the same as those with bulk gels, except that supercritical drying with CO₂ was carried out prior to calcination. Supercritical drying produced sticky aerogels that still contained significant amounts of residual organic matter. K–birnessite or cryptomelane were obtained after calcination, depending on the K:Mn dopant level. XRD patterns for the materials were the same as those from bulk gel syntheses. BET surface area measurements revealed a substantial increase in surface area over the regular sol–gel workup. K–birnessite registered a surface area increase from 24.2 to 39.3 m²/g due to supercritical drying, while the surface area of cryptomelane improved from 10.8 to 23.4 m²/g. However, despite these large relative increases, the absolute surface areas of the manganese oxides were unexceptional.

SEM images of K–birnessite and cryptomelane from calcined aerogels are shown in Figure 14. The effect of supercritical drying was particularly evident for K–birnessite, which had a lamellar appearance that differed significantly from the globular particles seen previously (Figure 3) from a regular workup of the bulk gels. Cryptomelane particles were still fibrous after supercritical drying, but the fibers appeared shorter than those observed with the regular sol–gel workup (Figure 5).

The surface area measurements on K–birnessite and cryptomelane indicate that supercritical drying can be effective in increasing the porosity of the gel matrix. This, in turn, results in higher surface areas for the calcined manganese oxide products, though not to an exceptional level. The nature of the nonaqueous gel matrix is likely to hinder the formation of very high surface area materials. Classic aerogels, such as those for SiO₂ and TiO₂, are prepared by alkoxide condensation, so the gel matrixes have direct oxygen links between the metal or semi-metal sites.⁴⁷ The oxide framework is therefore established before supercritical drying and solvent extraction can be accomplished without major disruption to the structure. This promotes the formation of materials with exceptionally high surface areas. By contrast, the manganese oxide gel matrix contains a high level of residual organic material that is nonvolatile and cannot be extracted by supercritical drying. This results in sticky aerogels with undefined manganese oxide frameworks. The organic material is combusted upon calcination, causing considerable weight loss (>60%), collapse of the porous structure, and lower surface areas for the products. This is an inherent drawback of the redox sol–gel approach.

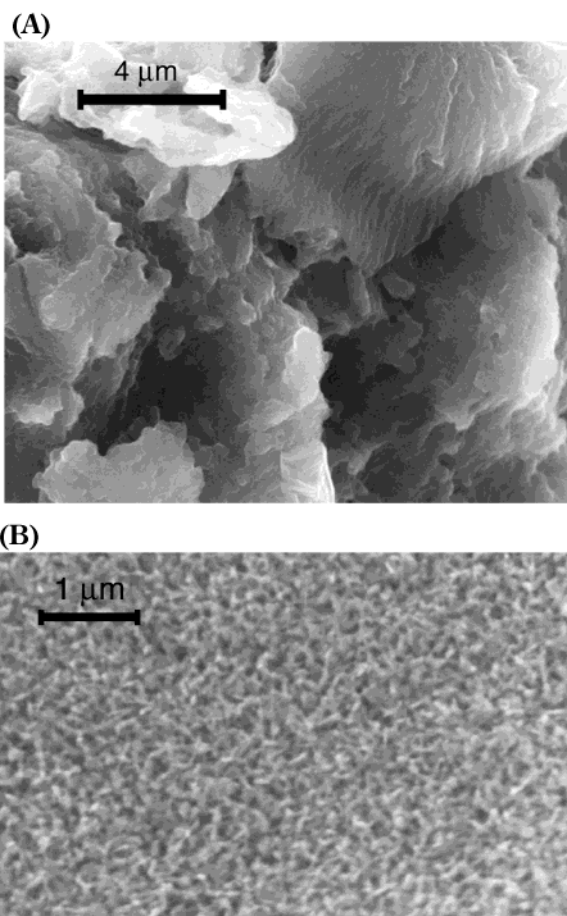


Figure 14. SEM images of (A) K–birnessite and (B) cryptomelane prepared from calcined aerogels.

However, recent aerogel work with aqueous sol–gel syntheses shows that high surface area manganese oxides can be achieved.^{48,49}

Conclusions

We have developed viable, nonaqueous sol–gel routes to microporous manganese oxides with birnessite, cryptomelane, and spinel structures. Gels are easily obtained from redox reactions involving TBAMnO₄ or TEAMnO₄ in methanol. Alkali-metal cations play a key role as dopants/templates for the microporous frameworks. The nonaqueous process has been successfully applied to the preparation of manganese oxide thin films and aerogels, thus utilizing the advantages of sol–gel chemistry. We are conducting further investigations in the areas of thin films and aerogels.

Acknowledgment. We are grateful for the generous support of the Research Corporation and the donors of the Petroleum Research Fund, administered by the American Chemical Society. We also wish to thank the Keck Foundation for providing undergraduate summer fellowships for E.J.W., S.M.H., and A.B.F.B.

CM010780Q

(45) Pang, S. C.; Anderson, M. A. *J. Mater. Res.* **2000**, *15*, 2096.

(46) Giraldo, O.; Brock, S. L.; Willis, W. S.; Marquez, M.; Suib, S. L.; Ching, S. *J. Am. Chem. Soc.* **2000**, *122*, 9330.

(47) Husing, N.; Schubert, U. *Angew. Chem., Int. Ed.* **1998**, *37*, 22.

(48) Long, J. W.; Swider-Lyons, K. E.; Stroud, R. M.; Rolison, D. R. *Electrochem. Solid State Lett.* **2000**, *3*, 453–456.

(49) Long, J. W.; Stroud, R. M.; Rolison, D. R. *J. Noncryst. Solids* **2001**, *285*, 288–294.